



Charged particle motion in spatially varying electric and magnetic fields

J.A. Young, C.M. Surko *

Department of Physics, University of California, San Diego, 9500 Gilman Drive, La Jolla, CA 92093-0319, USA

Available online

Abstract

The motion of charged particles in spatially varying electric and magnetic fields is studied using computational and analytic techniques. The focus of the work is determination of the circumstances for which an adiabatic invariant, defined as the ratio of the energy associated with the particle gyromotion to the local magnetic field strength, is a constant. When it is constant, this quantity is extremely useful in understanding particle motion in a range of applications. This study uses as an example the motion of positrons in spatially varying electric and magnetic fields typical in recent low-energy scattering experiments. The relationship of these considerations to other physical situations is briefly discussed.

© 2006 Elsevier B.V. All rights reserved.

PACS: 41.75.Fr; 45.50.-j; 52.65.Cc

Keywords: Positron beams; Positron scattering; Particle beams; Non-adiabatic effects

1. Introduction

There are many situations in which one would like to have precise knowledge of the motion of charged particles in electric and magnetic fields. Examples involving positrons include the accumulation of positrons in Penning–Malmberg traps, the formation of cold, trap-based beams and the use of spatially varying magnetic fields to make a variety of low-energy scattering measurements [1,2]. Similar considerations are important in the formation and manipulation of beams from intense positron sources such as those from nuclear reactors or electron linear accelerators (LINACs) [3], or to produce specially tailored beams for a range of applications [4,5]. In the case of spatially varying fields, when the time-variation of the fields is sufficiently slow in the frame of the moving particle, one can make use of an adiabatic invariant,

$$\xi \equiv \varepsilon_{\perp}/B, \quad (1)$$

where ε_{\perp} is the energy associated with the gyromotion of the particle about the magnetic field of local strength B , to predict the velocity components of the particle [6]. The invariance of ξ can be derived via an action-angle formalism and is linked to other invariants such as the magnetic moment and the flux through a particle orbit [6]. Qualitatively, if the fields vary slowly compared to the cyclotron period $\tau_c = 2\pi mc/eB$, one can expect that ξ is approximately constant. In this paper, we explore this issue quantitatively, elucidate situations in which ξ is invariant to a high degree of accuracy and those in which it varies significantly.

An important challenge in positron atomic and molecular physics is precise determination, at high-resolution, of low-energy scattering cross sections [2], and we use this physical situation as an example. In particular, we have developed a technique to measure these cross sections that relies on understanding in detail the motion of a charged particle in spatially varying electric and magnetic fields [7,8]. This scattering technique has proven superior to conventional methods, for example, in measuring integral inelastic scattering cross sections. It is most simply applied

* Corresponding author. Tel.: +1 858 534 6880; fax: +1 858 534 6574.
E-mail address: csurko@ucsd.edu (C.M. Surko).

when one can assume that ζ is a constant of the positron motion; testing this assumption motivated the present study.

We describe the results of computer simulations designed to test the invariance of ζ in this and similar situations [9]. While we focus on positrons, the results also apply to electrons, albeit with the appropriate change of sign, or to ions with appropriate change in mass. The considerations discussed here are relevant, for example, for positron (or electron) scattering processes at energies ~ 0.1 – 100 eV, such as near-threshold studies of vibrational and electronic excitation and searches for narrow resonances. They will be especially important in processes at millivolt energies, such as the roto-vibrational excitation of molecules.

2. Example of low-energy positron scattering using a trapped beam

Recent positron scattering experiments [7,8,10–12] use a ^{22}Na source, solid neon moderator and Penning–Malmberg trap to produce a relatively intense, monoenergetic pulsed positron beam. A buffer gas is used to trap and cool the positrons to ambient temperature (i.e. 25 meV at room temperature) [1]. An axial magnetic field ensures radial confinement of the charged particles. Cylindrical electrodes produce electrostatic potentials that confine the particles axially. Positrons are ejected from the trapping well by raising the well potential until positrons spill over the electrostatic barrier that is the exit gate of the trap. The voltage of this barrier determines the energy of the positron beam. For trap electrodes at room temperature, the parallel energy spread of the beam can be as small as 18 meV [13] and thus provides an excellent source for scattering experiments.

Normal operation of the scattering experiment assumes ζ is constant and that the magnetic and electrical potentials can be varied slowly so as to preserve the separation of the energies in the perpendicular and parallel degrees of freedom, except in collisions. Energy conservation dictates that any change in the electrical potential will be compensated by an equal change in the parallel kinetic energy of the particle. Thus, if the energy of the particle in the trap and the spatial dependence of the electric and magnetic fields are known, the particle may be injected into regions such as gas cells (e.g. used in scattering and annihilation experiments) with known values of parallel and perpendicular kinetic energy. A scattering event with an atom or molecule takes place on a spatial scale of the order of the Bohr radius, $a_0 = 0.53 \times 10^{-8}$ cm, which is much smaller than the positron gyroradius, $\rho \sim 10^{-3}$ cm. Thus, one can regard the scattering event as resetting the parallel and perpendicular energy (and hence ζ), and then follow the subsequent motion of the particle in the adiabatic limit.

As a case study of the invariance of ζ , we consider in detail what turns out to be the most critical test of ζ invariance in the scattering experiment shown in Fig. 1. The

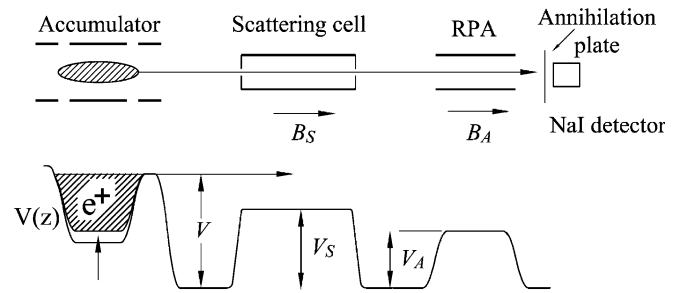


Fig. 1. Schematic diagram of a positron scattering experiment using a magnetically guided beam [7,8]: (above) arrangement of the electrodes and detector and (below) the on-axis electrical potential. A monoenergetic positron beam is guided through the scattering cell and then through a retarding potential analyzer (RPA). The magnetic field strength in the scattering cell and RPA, B_S and B_A , can be varied independently. If ζ is invariant, and $B_S \ll B_A$, the perpendicular energy ε_{\perp} in the analyzer will be small, and the RPA can be used to measure the total particle energy, ε .

apparatus consists of a scattering cell and a retarding potential analyzer (RPA) in magnetic fields B_S and B_A that can be varied independently. Positrons of known energy are magnetically guided into a gas cell where they interact with a known pressure of test gas. The kinetic energy of the positrons in the cell is varied by applying a voltage to the cell. The positrons in the cell may either collide elastically or inelastically (including forming positronium atoms, in which case, they are lost from the beam). In a scattering event, some of the positron's parallel kinetic energy can be redistributed into the perpendicular direction. The parallel energy distribution of the positrons exiting the scattering cell can then be measured using the RPA. If the magnetic field in the RPA is identical to that in the scattering cell, one cannot distinguish between elastic and inelastic processes as both can result in a loss of parallel energy. However, if one significantly reduces B_A relative to B_S , the invariance of ζ means that ε_{\perp} will be reduced proportionately. In this way, the distribution of parallel energies in the RPA can be made close to the distribution of total particle energies and hence be used to measure the energy loss associated with inelastic scattering events.

The simplest form of analysis of scattering data assumes that ζ is constant except during the scattering event [7,14]. The study described here tests this assumption, focusing on the region near the entrance to the scattering cell where rapidly varying electric fields can potentially affect ζ significantly. In positron scattering experiments such as that illustrated in Fig. 1, there are other places where the invariance of ζ can be questioned (e.g. when positrons from the moderator enter the Penning–Malmberg trap electrodes), but they are not as critical in determining the cross section as the analysis associated with positron orbits in the vicinity of the scattering cell.

In historical perspective, we were also motivated to further check the adiabatic assumption after observing unexplained anomalies in the cutoff voltages for our scattering cells. Nominally, the beam transport energy in the region between the trap and scattering cell can be determined by

measuring the cutoff energy in the scattering cell. This is obtained by raising the cell potential, V_S , until the beam is reflected. One can also measure the time of flight of a positron pulse as a function of cell voltage. Aided by computer models of the axial electrical potential, one can then fit the time of flight data to determine the transport energy. In practice, the two measurements have been found to differ by as much as 50–100 meV [15]. This discrepancy was a motivation for the present study, namely to determine if unanticipated variations in ξ could explain the observations. We found however that the adiabatic assumption appears to be correct (i.e. ξ is constant) for the experiments conducted to date. Thus, the origin of the anomalous behavior is still under investigation.

In this paper, we explore under what circumstances the adiabatic assumption is valid and under what circumstances it can be expected to break down for the specific case of the scattering geometry described above. As an example of the richness of the problem, there are significant radial components to both the electric and magnetic fields in the narrow region of the scattering cell aperture. In such fields, the type of instantaneous acceleration experienced by the particle depends strongly on the instantaneous angle of its velocity vector. The key question is to what degree parameters such as the electrode potential bias, particle energies and proximity of the positrons to apertures affect the invariance of ξ . The analysis presented here seeks to answer these questions and to further elucidate prominent dynamical features in positron motion such as the nature of the cyclotron orbits and $E \times B$ drifts that arise when the electric field E is not collinear with B . In this regard, an analytical model is described that has proven useful in elucidating variations in ξ . Finally, we describe rudimentary estimates of weak breaking of the invariance of ξ and discuss qualitatively where one might expect more significant variations in this quantity.

3. The model and computer simulations

3.1. Description of the calculations

The physical situation studied here is the nature of positron orbits in the vicinity of the scattering cell shown in Fig. 1. We assume the non-uniform magnetic field shown in Fig. 2, which is symmetric about the z -axis. The solenoid that contains the simulated scattering-cell electrode is 60 cm long and produces a field of 1 kG. The magnitude of the field drops to 140 G in the region between the buffer-gas trap and the scattering cell. The scattering cell electrode is 43 cm long. The ungrounded region is approximately 38.1 cm long and centered on the small solenoid, with circular apertures of radius $a = 0.254$ cm at each end. The scattering cell is at a positive potential with respect to the vacuum chamber, which is at ground.

The simulations presented here are numerical integrations of the fully relativistic Lorentz equations. This was required to achieve millivolt accuracies for ξ and other

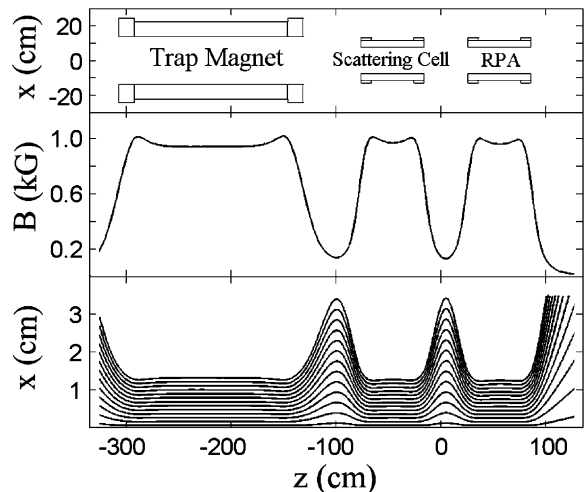


Fig. 2. Magnetic field model for the scattering experiment: (upper) placement of the solenoid magnets; (middle) magnetic field strength along the axis of symmetry and (lower) examples of field lines at various initial radii, x . The z -axis coordinate has an arbitrary offset compared to that in Fig. 3 below.

relevant quantities. The three-dimensional electric and magnetic fields were determined directly from simplified models of the electrodes and electromagnets via a PDE solver in MATLAB. The simulations consider only the motion of single particles and hence neglect any possible plasma dynamics and beam-induced image charges in the conductors.

The calculation was done using MATLAB. The numerical integrations were passed through the robust built-in solvers `ode15s` and `ode45`. The electrode potentials were modeled in PDETOOL exploiting cylindrical and mirror symmetries. A 1 Volt normalized solution was calculated on an adaptive triangular mesh and exported into a uniform square mesh, typically with 0.005 cm spacing. This initial conversion was computationally costly, but in the long term saved time in the particle motion integration stage. The model electrode and the solution for the electrostatic potential are shown in Fig. 3. A customized routine generated the magnetic field arrays. Array interpolations were done with a simple 4-point bilinear scheme.

We use an absolute coordinate system whose axial direction is the z -axis. In uniform magnetic fields, “parallel” and “perpendicular” refer to this axis. A positron whose cyclotron center is initially on the z -axis continues in the $+z$ direction while gyrating in the (x, y) plane. All initial radial offsets are taken to be in the $+x$ direction and initial velocities in the $+y$ direction. Later in this paper, a field-line coordinate system is introduced whose instantaneous z -axis is along the direction of the local magnetic field. For reasons to be explained later, this will become the new reference for “parallel” and “perpendicular”, while the absolute coordinates will still be used for describing position. The simulations consider only the change in orbits of particles entering the cell. By symmetry, similar effects are expected for particles exiting the cell.

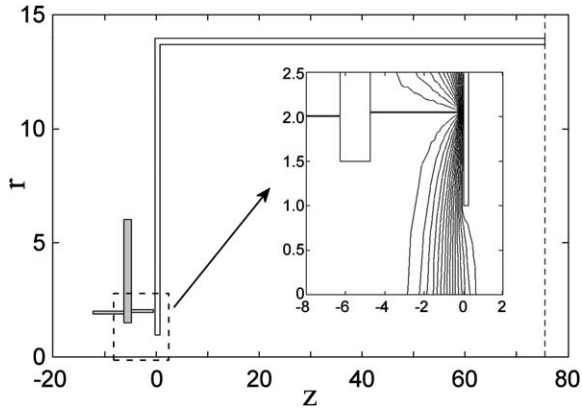


Fig. 3. Schematic of the scattering cell and electrical potential distribution. The unshaded electrodes are at a potential V_S and the shaded electrodes are at ground. Dimensions are in units of the aperture radius, $a = 0.254$ cm. The vertical dashed line represents the reflection plane of the cell; some components have been expanded to aid visibility. The inset is a close-up view of the region near the entrance aperture, with lines indicating 16 equally spaced equipotential contours.

3.2. Error-producing effects

These simulations involved millions of iterations due to the highly oscillatory nature of cyclotron motion and to avoid non-physical drifts as a result of over-extrapolation. If the step size was too small, the computation time became prohibitively long. Energy conservation was verified, and this exercise proved quite instructive. The original assumption for the total particle energy, ε , was the non-relativistic expression, $\varepsilon = \frac{1}{2}mv_{\perp}^2 + \frac{1}{2}mv_{\parallel}^2 + eV$. In the case of a positron with 90 eV parallel energy and 25 meV perpendicular energy moving from ground into an 85 V potential, energy was almost, but not quite conserved. There was an apparent loss of 8 meV in the region of the interface between ground and the applied potential. This error was, in fact, due to the non-relativistic approximation. For this reason, all further calculations used fully relativistic particle dynamics and energy equations. We note that, for experimental positron beams much colder than room temperature, this effect could be important in the energy accounting.

A small, gradual loss of energy was observed as the simulation progressed. This was a numerical error as it could be corrected by increasing the minimum accuracy of each numerical step (e.g. by reducing step size). The energy loss during a typical trial could be reduced below 0.1 meV if adaptive 10 ns steps were used.

Another check of accuracy is the variation of the gyroradius and gyrofrequency as a function of magnetic field strength. The simulations were first performed with a constant axial magnetic field of 1 kG and an initial perpendicular energy of 0.025 eV. The helical motion conformed nearly perfectly to this prediction, except at the interface of the electrodes where electric fields produced a deflection in the y (azimuthal) direction of the guiding center of the helical particle orbits. The size of this deflection was typi-

cally a few gyroradii (i.e. $\rho \sim 5 \times 10^{-4}$ cm for $\varepsilon_{\parallel} = 90$ eV and $B = 1$ kG). Evolution of the y coordinate for several different initial radial positions is shown in Fig. 4. The aperture of the electrode was $a = 0.254$ cm in radius and the axial distance from ground to half the electrode voltage was also ~ 0.25 cm. Our conclusion is that small radial electric fields, which are most pronounced near the edges of the apertures, create the observed orbit deflections.

In the electric field-free region just outside of the electrode, the particles follow the magnetic field lines to within a cyclotron gyroradius, expanding to large radii at low field and narrowing at large field. The perpendicular energy varies according to the adiabatic invariant, $\xi = \varepsilon_{\perp}/B$, with tighter gyrations at higher magnetic field.

When the complete magnetic field was used, new behavior was observed: close inspection of ε_{\perp} (i.e. the energy in the (x, y) plane) as a function of axial position revealed a slight wobble at the cyclotron frequency. A similar wobble occurred in E_z because of energy conservation. This effect increased as the particle motion was displaced further off-axis, reaching an amplitude of 25 meV for particles passing near the aperture edge at a transport energy of 85 eV. This was due to the choice of coordinate system. The particles move along the magnetic field lines, which are not exactly parallel to the z -axis. An appropriate rotation eliminated this wobble and revealed a remarkably constant value of ξ in regions of constant voltage. To add consistency to later simulations, the initial conditions for transport were framed in terms of local field-line coordinates. The initial “perpendicular” energy was set such that it would be 25 meV in a 1 kG field regardless of initial position. This corresponds to an initial value of $\xi_i = 25$ meV/kG outside the cell.

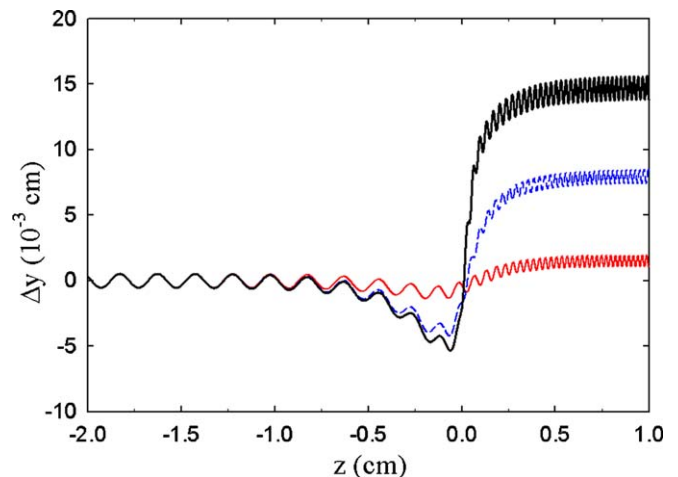


Fig. 4. Deviation, Δy , of the azimuthal coordinate for different initial radii, x_i , as a function of distance from the aperture located at $z = 0$. Note that Δy increases close to the aperture. The rapid oscillations are due to the cyclotron motion, while the larger excursions are due to an $E \times B$ drift. In terms of the aperture radius, a , the curves are: (—) $r_i = 0.2a$; (---) $r_i = 0.8a$ and (heavy line) $r_i = 0.95a$.

4. Numerical results

Unexpected effects occur when the electric potential is not constant. In extreme cases, the adiabatic invariant is broken by many tens of meV/kG. An example is shown in Fig. 5. The dashed line is the lab frame result. Note the large amplitude oscillations that occur at the cyclotron frequency close to the edge of the electrode. If one examines the adiabatic invariant in the $E \times B$ drift frame, one finds that these oscillations practically disappear, as shown by the solid line in Fig. 5.

However, while these large oscillations can be eliminated, *the actual breaking of the adiabatic invariant cannot be eliminated*. The magnitude and direction of this “shift” varies sinusoidally with the initial angle, θ_0 , between the perpendicular velocity component and the x -axis. This angle θ_0 is a measure of the initial phase. This sinusoidal variation is sufficiently large that it cannot be ignored. Ultimately, we would like to know how the final parallel energy distribution compares to the experimentally determined “cutoff” distribution. To do this, we need to examine all initial radii and phases.

To better quantify the observed variations in ξ with phase, we define the average value, $\bar{\xi} \equiv (\xi_+ + \xi_-)/2$, and the peak sinusoidal variation, $\Delta\xi \equiv (\xi_+ - \xi_-)/2$, where ξ_+ and ξ_- are respectively the maximum and minimum values of the final adiabatic invariant over a 2π change in phase. With all other parameters held fixed, a batch of 11 initial phases were used to determine ξ_+ and ξ_- . If the adiabatic invariant were conserved, the average would be the initial value, namely $\bar{\xi} = 25$ meV/kG, and $\Delta\xi = 0$. In our plots, we normalize $\bar{\xi}$ and $\Delta\xi$ to the initial value $\xi_i = 25$ meV/kG to give unitless parameters. This is merely a convenience and is not meant to indicate scale invariance. In fact,

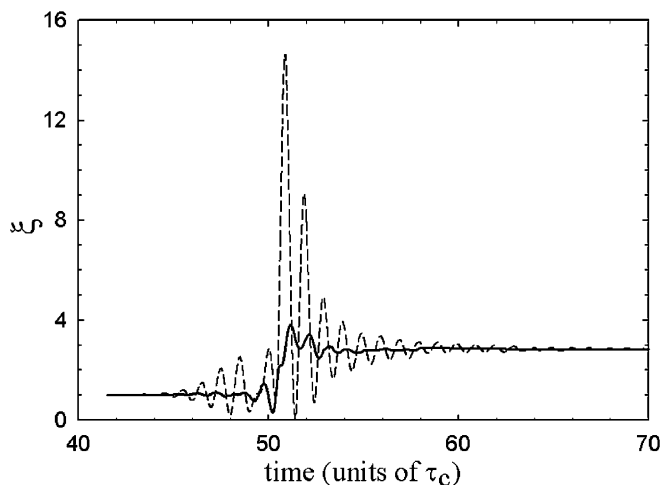


Fig. 5. Example of breaking of the adiabatic invariant, $\xi = \varepsilon_{\perp}/B$. A positron with $\varepsilon_{\parallel} = 90$ eV, $\varepsilon_{\perp} = 0.025$ eV, $y = 0.95a$, and arbitrary initial phase enters a scattering cell at an electrical potential of 89 V in a uniform 1 kG field. The vertical axis is normalized to the initial value, $\xi_i = 25$ meV/kG, and time is given in units of the cyclotron period, τ_c : (---) ξ in the lab frame; and (—) ξ with the $E \times B$ drift removed (i.e. the drift-frame value).

as mentioned later, the above parameters actually scale better with changes in overall transport energy.

As illustrated in Fig. 6 for a 90 eV beam entering an 89.7 V cell, $\Delta\xi$ can increase dramatically close to the edge of the aperture. To parameterize the data for further analysis, we plot in Fig. 7 the data from Fig. 6 as a function of radial distance from the aperture on a log–log scale. The data can be fit by the form

$$\Delta\xi = b/(1 - x/a)^2 + c, \quad (2)$$

where a is the aperture radius; $b = 8.4 \times 10^{-2}$ and $c = 3.0$, with both in units of meV/kG. The ‘phase-average’, $\bar{\xi}$, follows a nearly identical trend, diverging as $1/(\Delta x)^2$, where Δx is the distance from the aperture. Generally, it is found that the change in $\bar{\xi}$ is almost equal to $\Delta\xi$.

The parameters $\bar{\xi}$ and $\Delta\xi$ appear to diverge at the aperture for all cell voltages except zero. As the cell voltage rises

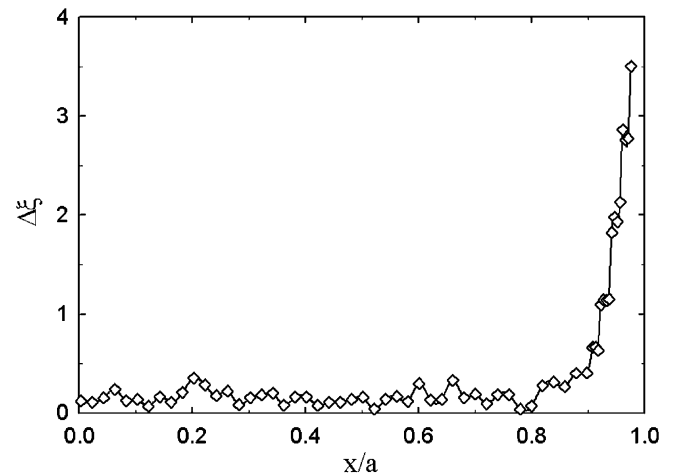


Fig. 6. Adiabatic invariant breaking parameter, $\Delta\xi$ (normalized to the initial value, $\xi_i = 25$ meV/kG), shown as a function of initial radial offset, x/a (where a is the aperture radius), for a positron with $\varepsilon_{\parallel} = 90$ eV and $\varepsilon_{\perp} = 0.025$ eV entering an 89.7 V cell in a 1 kG magnetic field.

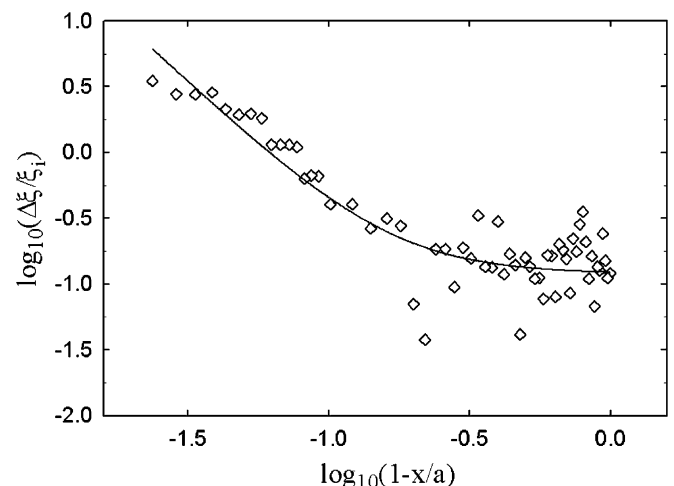


Fig. 7. Power law behavior of $\Delta\xi/\xi_i$ observed near an aperture: (open diamonds) data from Fig. 6 on a log–log plot, where a is the aperture radius; and (—) fit to the data of the form $\Delta\xi = b/(1 - x/a)^2 + c$. See text for details.

from zero, the shifts near the aperture first increase, then level off when the cell voltage is within a few percent of the transport voltage. For example, the shifts for a 90 eV particle entering a cell at 85 V are similar to those entering a cell at 89.7 V. The only difference is that, in the later case, particles with more than 300 meV of perpendicular energy will be reflected due to energy conservation.

In the experiment, the parallel energy distribution is usually determined by measuring the intensity of the beam through the cell as the cell potential is raised above the transport or “cutoff” voltage. We call this derived energy distribution the “cutoff distribution”. This distribution is not necessarily identical to the true energy distribution as determined by our simulations. Close to cutoff, the two energy distributions are nearly equal. However, far from cutoff, where there is relatively little effect due to the interface, the true energy distribution is narrower than the cutoff distribution.

To determine the cutoff distribution, we use the fact that ξ varies sinusoidally with phase. Assuming all initial phases θ are equally probable, the amplitude $\Delta\xi$ and offset $\bar{\xi}$ can be used to calculate a weighted distribution of ξ for a given set of initial conditions. At fixed radius r , the probability $h(\xi, r)$ for a given final adiabatic invariant ξ is proportional to the change in phase, $\delta\theta$ associated with a small fixed change in the final adiabatic invariant $\delta\xi$. This can be expressed as

$$\begin{aligned} h(\xi, r)\delta\xi &= \frac{\delta\theta}{\pi} = \frac{1}{\pi} \frac{\partial\theta}{\partial\xi} \delta\xi \\ &= \frac{1}{\pi} \left[\sin^{-1} \left(\frac{\xi - \bar{\xi}(r)}{\Delta\xi(r)} \right) - \sin^{-1} \left(\frac{\xi - \delta\xi - \bar{\xi}(r)}{\Delta\xi(r)} \right) \right] \delta\xi. \end{aligned} \quad (3)$$

For a uniform beam of particles the probability distribution, $P(\xi)$ for ξ is then given by

$$P(\xi) \propto \sum_j h(\xi, r_j) \cdot r_j. \quad (4)$$

The values of $\Delta\xi(r)$ from Fig. 7 and similar values of $\bar{\xi}(r)$ (not shown) were used to construct the distribution $P(\xi)$ for the case of a 90 eV beam into 89.7 V cell, which is shown in Fig. 8. Also shown is the distribution acquired from the fit function in Fig. 7.

The distribution is centered on the original adiabatic invariant value, 25 meV/kG with an approximate flat top of width ~ 8 meV/kG, FWHM. There is a long high-energy tail that extends to 300 meV/kG where reflection occurs due to insufficient parallel energy. While large amplitude variations of the adiabatic invariant *do occur* near the aperture, few particles in the beam actually have shifts of this magnitude. Thus, these particles do little to shift the peak of the distribution, although the mean increases by a few meV/kG.

The fit-based distribution in Fig. 8 emphasizes the width of the distribution but is too sharply bimodal. The flat top

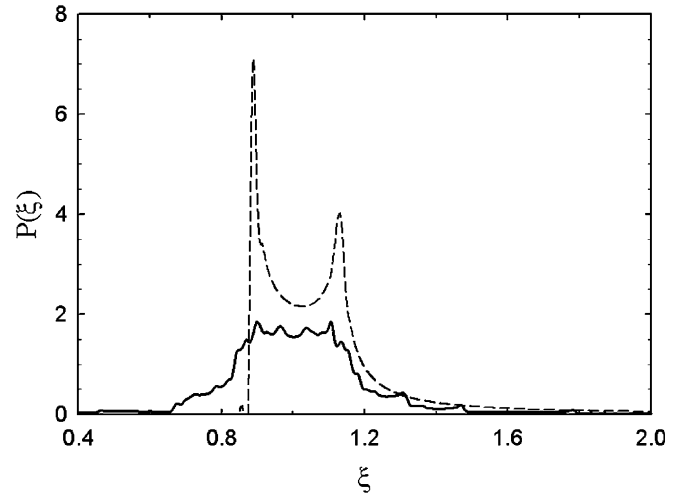


Fig. 8. Normalized distribution function, $P(\xi_i)$, for a uniform beam of particles with arbitrary initial phases, where ξ is in units of the initial value, $\xi_i = 25$ meV/kG. The distribution is calculated using data for $\Delta\xi(r)$ from Fig. 6 and similar data for $\bar{\xi}(r)$: (—) simulated data; and (---) using the fit to $\Delta\xi(r)$ from Fig. 7 and a similar fit to $\bar{\xi}(r)$.

feature is due to the significant variation of amplitudes at smaller radii illustrated in Fig. 7. (It is presently unclear whether these amplitudes are due to small amounts of numerical noise or whether they are due to some aspect of particle dynamics for this class of orbits.) Note that, in an actual experiment, a positron beam will have a distribution of parallel and perpendicular energies even before entering the cell. To determine the distribution of positrons transmitted through the cell (i.e. with no test gas), this must be convolved with the distribution of non-adiabatic perturbations described above and then convolved with the distribution due to non-adiabatic effects experienced by positrons exiting the cell.

Two further remarks are in order. Results from simulations using the actual non-uniform magnetic field model do not differ significantly from those of the uniform 1 kG field. Also, it was found that adiabatic breaking is significantly reduced at lower transport energies. In this case, most of the significant shifts occur so close to the edge of the aperture that lack of resolution makes it difficult to fit the data. Preliminary indications show that the power law may actually change at low values of transport energy.

5. Analytical description

The question yet to be addressed is the actual origin of these effects. The magnitude of the electric force orthogonal to the magnetic field direction $E_{\perp} = |\vec{E} \times (\vec{B}/B)|$ is large near the face of the electrode. When this force is perpendicular to the velocity, the inward acceleration results in a change in cyclotron radius. When the force is parallel or antiparallel to the velocity, this radial velocity component will increase or decrease. One consequence of these effects is an $E \times B$ drift in the azimuthal direction. If the radial electric field is relatively constant, the gains and losses in perpendicular energy will be phase-averaged away.

However, if the field is large and varies greatly over a few cyclotron gyrations, the cumulative effect on the perpendicular energy (and hence the ξ) can be non-negligible.

In order to predict the breaking of the adiabatic invariant, we take the integral of these perpendicular energy gains and losses along a field line. To a good approximation, the parallel velocity can be determined from the transport energy minus the local value of the electrical potential. The angle of the velocity with respect to the orthogonal electric field changes at the (near constant) cyclotron frequency. Spatial drifts can be ignored as small and neither radial nor axial. A good quantity to integrate is an adiabatic invariant closely related to ξ , v_{\perp}/\sqrt{B} :

$$\frac{v_f}{\sqrt{B_f}} = \frac{v_i}{\sqrt{B_i}} + \int \frac{1}{\sqrt{B}} \frac{dv}{dz} dz. \quad (5)$$

Note that there is no dB/dz term. At this order, invariance protects against change due to a varying magnetic field. However, accelerations resulting from the non-magnetic force of the electric field, which are time-varying in the frame of the moving particle, are important and must be treated explicitly. In particular,

$$\Delta\left(\frac{v_{\perp}}{\sqrt{B}}\right) = \int_{\hat{B}} \left[\frac{1}{\sqrt{B}} \cdot \frac{eE_{\perp}}{m} \cdot \cos(\theta(z)) \right] dt, \quad (6a)$$

where

$$\theta(z) \cong \int \frac{\omega_c dz}{v_z} + \theta_0, \quad v_z = \sqrt{\frac{2(\varepsilon_{\parallel} - e \cdot V)}{m}}, \quad \text{and} \quad \omega_c = \frac{eB}{mc}, \quad (6b)$$

with θ_0 the initial phase. The integrals in Eqs. (6a) and (6b) are taken along a magnetic field line. This expression provides reasonable predictions in “low” electric field regions where the percentage change in the adiabatic invariant are not too large.

Better precision can be achieved by using relativistically correct quantities. In this case, the adiabatic invariant quantity is $(p_{\perp}/m)/\sqrt{B}$. The axial velocity can be determined from the axial momentum,

$$v_z = \left(\frac{p_z}{m}\right) \left(\frac{mc^2}{\varepsilon}\right), \quad \text{where} \quad (7a)$$

$$\frac{p_z}{m} = \sqrt{\left[\left(\frac{\varepsilon_K}{mc^2}\right)^2 + 2\left(\frac{\varepsilon_K}{mc^2}\right)\right]c^2 - \left(\frac{p_{\perp}}{m}\right)^2}, \quad \text{and} \quad (7b)$$

$$\varepsilon_K = \varepsilon - mc^2 = mc^2 \sqrt{1 + \frac{1}{c^2} \left(\frac{p_0}{m}\right)^2} - e(V - V_0) - mc^2. \quad (7c)$$

The perpendicular momentum is now included in the calculation of v_z . As this parameter depends on the adiabatic invariant, an iterative calculation is possible. A zeroth-order treatment is sufficient for most small perturbations.

Another correction that becomes necessary when the $E \times B$ force is large has to do with the phase $\theta(t)$. Changes in speed depend on the dot product of the force and the

unit velocity vector. Thus far, it has been assumed that the angle of the velocity relative to the radial direction changes at the cyclotron frequency. However, if a small azimuthal drift is assumed, the sum of drift and cyclotron velocity vectors *do not* change angle at a constant rate. In fact, since forces and $E \times B$ drift go hand in hand, one can stifle the other. In this case the drift, which is perpendicular to the force, adds to the velocity component perpendicular to the force, thus reducing any possible changes in speed.

The approximate expression given by Eqs. (6) and (7) works reasonably well at most radii. The exact oscillations and the final value of the adiabatic invariant are consistent with those of the full simulation. However, ξ starts to deviate from the simulation when the particle is close to an electrode. In this case, the solutions become out of phase in high $E \times B$ regions, significantly altering the results. Even small phase variations can have significant consequences; comparison of the analytic approximation and that of the full simulation shows that as little as a tenth of a cycle phase shift can change the final shift. When the exact angle function is substituted for the approximate one, the resulting prediction matches the simulation flawlessly.

6. Summary

In this paper, we have discussed higher-order effects that affect the motion of charged particles passing through a configuration of electrodes in a strong magnetic field. Perturbations in particle motion are observed to occur at the edges of apertures due to rapid variations in E_{\perp} and $E \times B$. In most cases considered here, the perturbations result in only a few meV of positron energy shifting from the parallel to the perpendicular direction for changes in electrical potential ~ 90 V. Very generally, the adiabatic invariant, $\xi = \varepsilon_{\perp}/B$ is found to be constant to an appropriately high degree of accuracy for the situations relevant to previous scattering experiments using trap-based positron beams and the technique of scattering in a strong, spatially varying magnetic field [7,8,10–12].

With regard to higher-order effects, there is a high-energy tail in the final distribution for particles undergoing a rapid acceleration or deceleration and passing close to an electrode. While the size of this effect is small in the context of previous positron scattering measurements, it may play a more significant role in the future. For example, as the temperature of the beam is reduced, meV shifts can become more important, especially in low-energy and near-threshold scattering experiments.

These non-adiabatic shifts originate from the perpendicular electric forces acting on a particle gyrating in a magnetic field. Since any cancellation of the effect of these forces must take place over a cyclotron period or longer, it is not surprising that the adiabatic invariant is, at least temporarily, not conserved. Non-uniformity of the radial electric field over a cyclotron period then makes the energy shift permanent. The analytic description of this phenomenon (i.e. Eqs. (6)

and (7)) performs well as long as the adiabatic breaking is not too strong. However, for particles very close to electrodes, short-term adiabatic oscillations can have very high amplitudes. In this case, small, higher-order perturbations in phase can seriously affect the final result, leading to a breakdown of the analytic description.

We believe that the simulations described above have greatly clarified charged particle dynamics in such fields. Should it be necessary to further reduce breaking of the adiabatic invariant, ξ , the magnitude of the electric field must either be further reduced and/or made more uniform on the time scale of a cyclotron period. One solution is to keep the particles further away from electrodes by, for example, using a smaller radius beam well centered in the apertures of the electrodes. One physical situation that was not discussed here, worth further examination, is that in which the magnetic axis is tilted with respect to the axis of the electrodes. In this case, the component of the electric field perpendicular to the magnetic field will be larger and could possibly lead to further changes in the adiabatic invariant.

Acknowledgements

We wish to acknowledge helpful conversations with J.R. Danielson and J.P. Marler. This work is supported by the National Science Foundation, Grant PHY 02-44653.

References

- [1] T.J. Murphy, C.M. Surko, Phys. Rev. A 46 (1992) 5696.
- [2] C.M. Surko, G.F. Gribakin, S.J. Buckman, J. Phys. B: At. Mol. Opt. Phys. 38 (2005) R57.
- [3] C. Hugenschmidt, G. Kögel, R. Repper, et al., Rad. Phys. Chem. 68 (2003) 669.
- [4] C.M. Surko, R.G. Greaves, Phys. Plasmas 11 (2004) 2333.
- [5] A.P. Mills Jr., Nucl. Instr. and Meth. B 192 (2002) 107.
- [6] J.D. Jackson, Classical Electrodynamics, second ed., John Wiley Sons, New York, 1975.
- [7] S.J. Gilbert, R.G. Greaves, C.M. Surko, Phys. Rev. Lett. 82 (1999) 5032.
- [8] J.P. Sullivan, S.J. Gilbert, J.P. Marler, et al., Phys. Rev. A 66 (2002) 042708.
- [9] The case of a spatially uniform, but time-varying magnetic field is described in J.E. Borovsky, P.J. Hansen, Phys. Rev. A 43 (1991) 5605.
- [10] J. Sullivan, S.J. Gilbert, C.M. Surko, Phys. Rev. Lett. 86 (2001) 1494.
- [11] J.P. Sullivan, J.P. Marler, S.J. Gilbert, et al., Phys. Rev. Lett. 87 (2001) 073201.
- [12] J.P. Marler, J.P. Sullivan, C.M. Surko, Phys. Rev. A 71 (2005) 022701.
- [13] S.J. Gilbert, C. Kurz, R.G. Greaves, et al., Appl. Phys. Lett. 70 (1997) 1944.
- [14] J.P. Sullivan, S.J. Gilbert, J.P. Marler, et al., Nucl. Instr. and Meth. B 192 (2002) 3.
- [15] J.P. Marler, Ph.D. Thesis, University of California, San Diego, 2005, unpublished.